Nano Science and Technology Journal 1(1) 49-55 Summer 2023

RESEARCH PAPER

Synthesis, characterization and photocatalytic properties investigation of $CuFe_2O_4$/CdO nanocomposite

Kambiz Hedayati*[1]

[1]*Department of Science, Arak University of Technology, Arak, Iran*

Article History:
Received 18 August 2023
Accepted 21 September 2023
Published 22 September 2023

Keywords:
Nanocomposite
Photocatalytic
Ultrasonic

*Corresponding Authors Email:
k-hedayati@arakut.ac.ir

DOI: 10.22034/nstj.2023.707954

Abstract

In this article, copper ferrite ($CuFe_2O_4$) nanoparticles were synthesized by ultrasonic method without using surfactant. Cadmium oxide (CdO) nanoparticles were also synthesized without capping agent. After that, copper ferrite/ cadmium oxide nanocomposite was synthesized via ultrasonic method. Structural properties of synthesized $CuFe_2O_4$ and CdO nanoparticles and $CuFe_2O_4$/ CdO nanocomposite were studied using X-ray diffraction (XRD). The morphology of nanostructures was investigated by field emission scanning electron microscope (FESEM). The magnetic properties and hysteresis loop of the produced nanomaterials were investigated using a vibrating sample magnetometer (VSM). Finally, the photocatalytic properties of copper ferrite/cadmium oxide nanocomposite were studied using red acid and blue acid azo dyes.

1. Introduction

Ferrites are the main group of materials that have ferrimagnetic properties. ferrimagnetic materials, like ferromagnetic materials, have strong magnetic properties and are also electrically non-conductive. Ferrites have three main categories, namely, spinel ferrites, hexagonal ferrites, and garnet ferrites .Copper ferrite is one of the spinel ferrites. Spinel ferrites are known as soft ferrites [1-3].

Cadmium oxide is a semiconductor with an indirect band gap of about 1.4 eV and a monoclinic crystal structure [4-5].

Photocatalytic properties are mostly seen in semiconductors and metal oxides. Electrons of valence layer of semiconductors can be excited in the presence of UV rays and form an electron-hole pair. If these electron-hole pairs reach the surface of the photocatalyst material before recombination, they can react with the molecules around the surface and cause their oxidation and reduction. The combination of electron and hole with water and oxygen around the photocatalyst material can produce two functional groups, OH^{-} and O^{2-}, which are very reactive and by combining with hydrogen and carbon, they turn into toxic organic compounds. give water and carbon dioxide to non-hazardous materials [6-8].

Ferrite/semiconductor nanocomposites have many applications in the treatment of industrial effluents and degradation of azo dyes. Because semiconductor can cause photocatalytic properties and destruction of toxic substances due to visible light or ultraviolet radiation. After that, according to the magnetic property of ferrite, the nanocomposite can be removed from the water by a magnet [9-11].

In this research, ferrite nanoparticles were synthesized by ultrasonic method and its effect on the degradation of azo dyes under ultraviolet light was studied.

2. Experimental

2-1. Materials and methods

$Cu(NO_3)_2{\cdot}3H_2O$, $Fe(NO_3)_3{\cdot}9H_2O$, $Cd(NO_3)_2{\cdot}4H_2O$, NaOH, were purchased from Merck Co without further purifications. A multiwave ultrasonic generator with titanium oscillator, operating at 20 kHz and maximum power output of 1200 W was used for the ultrasonic irradiation. XRD patterns were investigated via a Philips PW3373CuKa (1.54 Å) radiation. FESEM images were obtained using an LMU TESCAN BRNO-Mira3. Room temperature magnetic properties were investigated using a VSMdevice (Meghnatis Kavir Kashan Co).

2-2. Synthesis of $CuFe_2O_4$ nanoparticles

0.32 g of $Fe(NO_3)_3{\cdot}9H_2O$ and 0.1 g of $Cu(NO_3)_2{\cdot}3H_2O$ were dissolved in 50 ml of deionized water. Then NaOH solution (1 M) was added to the solution under ultrasonic irradiation with a power of 1200 W and time cycles of 2 s of irradiation and 1 s of rest for 5 min. The pH of the solution was adjusted to 11. The obtained nanoparticles centrifuged and washed with deionized water. The product was dried in oven for 48 h and calcinated at 800 C for 2 h.

2-3. Synthesis of $CuFe_2O_4$/CdO nanocomposite

0.1g of synthesized $CuFe_2O_4$ was dispersed in 100 ml of water by ultrasonic irradiation (1200 W) for 10 min. Then 0.5 g of $Cd(NO_3)_2{\cdot}4H_2O$ was dissolved to 50 ml of deionized water and NaOH (1 M) was added to the solution. The solution is exposed to ultrasonic waves for 10 min (2 s of irradiation and 1 s of rest). The final product is centrifuged and washed, then dried in the oven for 48 h.

3. Result and discussion

The crystallite structure of $CuFe_2O_4$ nanoparticles and $CuFe_2O_4$/CdO nanocomposites was investigated via XRD. Fig. 1 shows XRD pattern of $CuFe_2O_4$ nanoparticles. The XRD pattern of $CuFe_2O_4$ corresponds to standard card JCPDS No.: 06-0545.

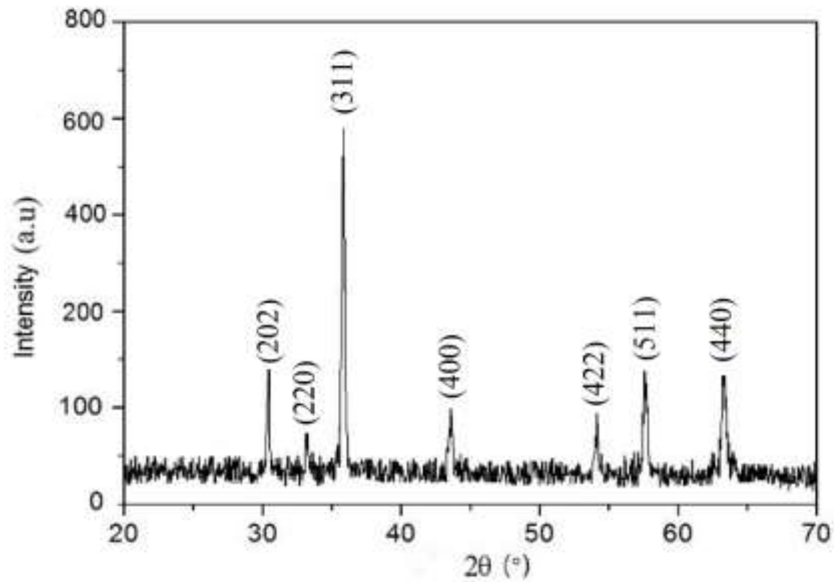

Fig.1. XRD patterns of $CuFe_2O_4$ nanoparticles.

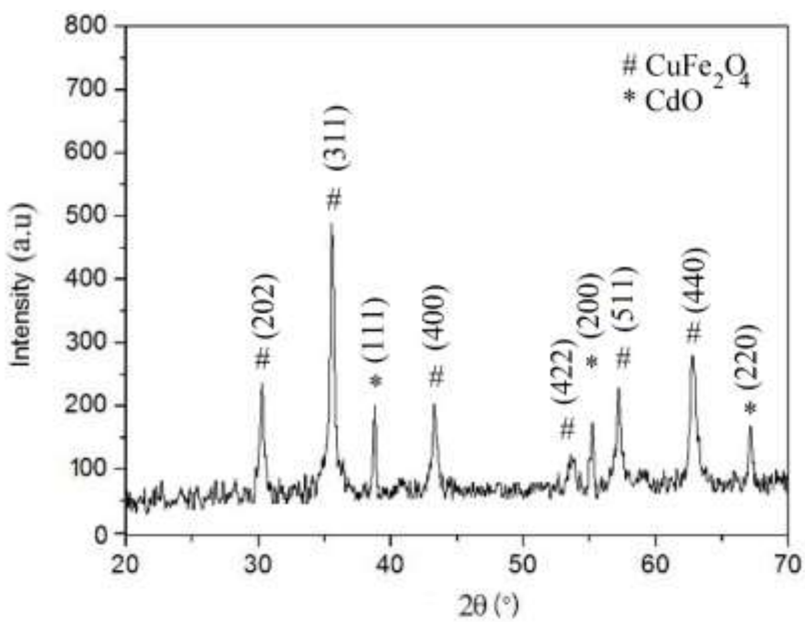

Fig.2. XRD patterns of $CuFe_2O_4$/CdO nanocomposites.

Fig .2 shows the X-ray diffraction pattern related to $CuFe_2O_4$/CdO nanocomposites. As can be seen in the Fig. 2, the peaks related to copper ferrite according to standard card JCPDS No.: 06-0545 and the peaks related to cadmium oxide according to standard card JCPDS No.: 01-1049 can be seen in the diffraction pattern, which indicates the formation of both phases in the composite.

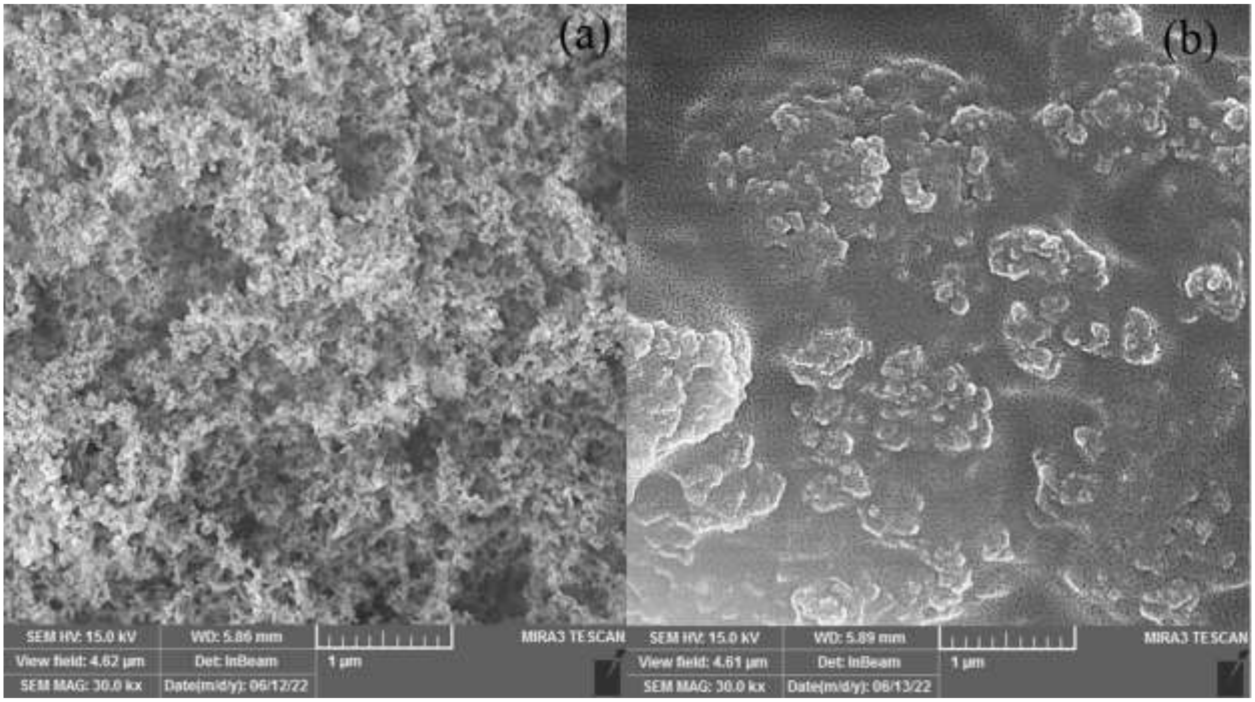

Fig.3. FESEM images of a) $CuFe_2O_4$ nanoparticles and b) $CuFe_2O_4$/CdO nanocomposites.

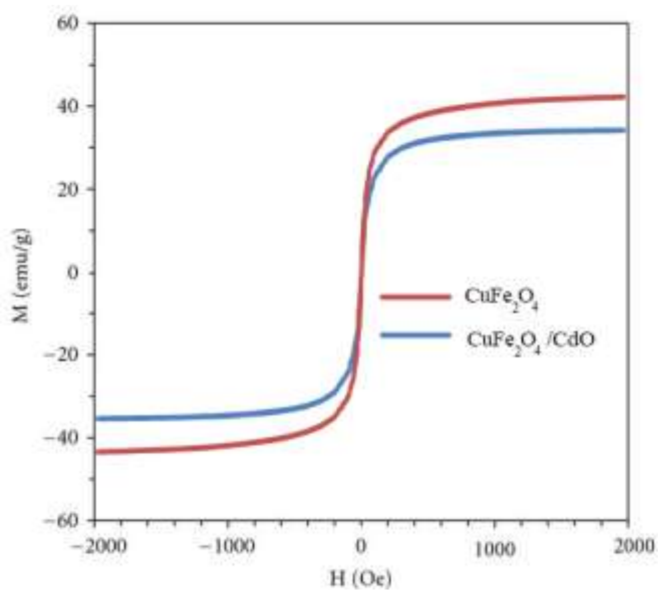

Fig.4. Hysteresis loop of $CuFe_2O_4$ nanoparticles and $CuFe_2O_4$/CdO nanocomposites.

The crystalline sizes of $CuFe_2O_4$ nanoparticles and $CuFe_2O_4$/CdO nanocomposites calculated via Scherrer equation, $Dc = K\lambda/\beta Cos\theta$, where β is FWHM, K is equal 0.9, and λ=0.154 nm [12] .The average crystalline size for $CuFe_2O_4$ nanoparticles and $CuFe_2O_4$/CdO nanocomposites were found to be about 28 and 36 nm respectively.

Fig .3 shows the field emission scanning electron microscope image of copper ferrite nanoparticles and copper ferrite/cadmium oxide nanocomposite. Fig .3 (a) shows the FESEM image of $CuFe_2O_4$ nanoparticles. This image clearly shows the synthesis of copper ferrite nanoparticles with a size below 50 nm. Fig .3(b) shows the FESEM image of the $CuFe_2O_4$/CdO nanocomposite. In this image, it is clear that copper ferrite nanoparticles are located in the cadmium oxide substrate. Also, the size of the grains in the $CuFe_2O_4$/CdO nanocomposites is larger than the size of the $CuFe_2O_4$ nanoparticles, which is consistent with the results obtained from X-ray diffraction for the crystalline size.

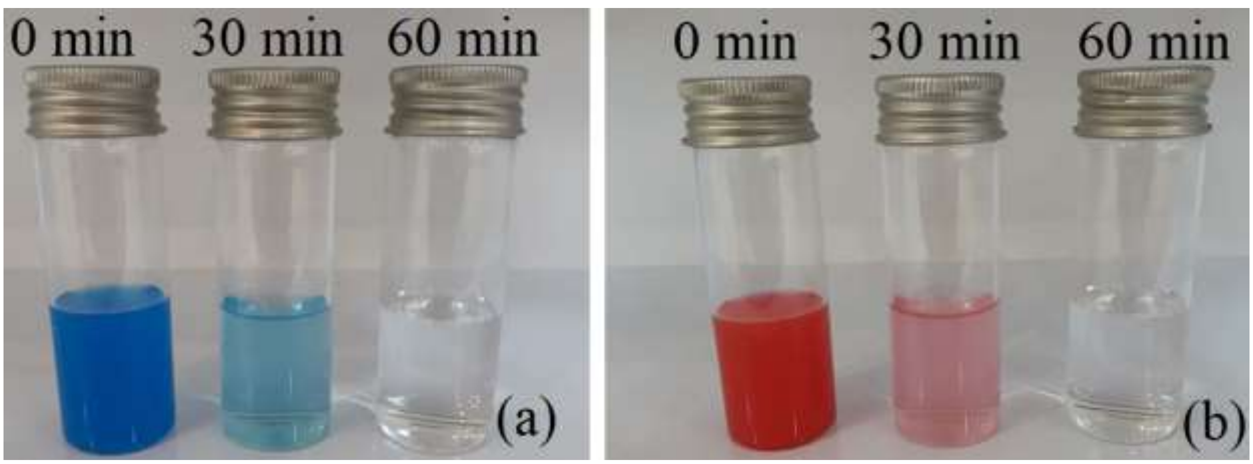

Fig.5. Photo-degradation of $CuFe_2O_4$/CdO nanocomposites a) acid blue b) acid Red.

The magnetic properties of $CuFe_2O_4$/CdO nanocomposites and $CuFe_2O_4$ nanoparticles were investigated using their hysteresis loop. According to Fig .4, both materials have superparamagnetic property and their hysteresis value is zero. As can be seen in the Fig. 4, the saturation magnetization of $CuFe_2O_4$ nanoparticles is equal to 43 emu/g and the saturation magnetization of $CuFe_2O_4$/CdO nanocomposites is equal to 35 emu/g. The reason for the decrease in saturation magnetization is the covering of copper ferrite nanoparticles by cadmium oxide nanoparticles.

To investigated the photocatalytic properties, 0.1 g of $CuFe_2O_4$/CdO nanocomposites was poured into 20 cc of blue acid and red acid solution and placed in a dark room under the radiation of 5 UV lamps with a length of 20 cm and a power of 8 W. As can be seen in Fig .5, after 60 minutes of UV irradiation, the colors of blue acid and red acid were destroyed, which shows the high photocatalytic power of this nanocomposite.

4. Conclusion

In this paper, $CuFe_2O_4$/CdO nanocomposite was synthesized by ultrasonic method without using surfactant and green synthesis method. X-ray diffraction patterns showed that the synthesized nanoparticles have a good match with the standard peaks. Also, the size of the obtained average crystalline for $CuFe_2O_4$ nanoparticles or $CuFe_2O_4$/CdO nanocomposites was calculated to be less than 50 nm. The FESEM image showed that the particles have nanometer size and $CuFe_2O_4$ nanoparticles are placed in the matrix of CdO nanoparticles. The magnetic hysteresis loop showed that $CuFe_2O_4$ nanoparticles and $CuFe_2O_4$/CdO nanocomposites have superparamagnetic properties and the saturation magnetization decreases with composites. Investigating the effect of ultraviolet light on red acid and blue acid in the presence of $CuFe_2O_4$/CdO nanocomposite showed the strong photocatalytic property of this nanocomposite.

References

[1] M. Ghobadi, Based on copper ferrite nanoparticles ($CuFe_2O_4$ NPs): Catalysis in synthesis of heterocycles, Journal of Synthetic Chemistry, 1(2) 2022, 84-96. https://doi.org/10.22034/JSC.2022.155234.

[2] A. Soufi, H. Hajjaoui, R. Elmoubarki, M. Abdennouri, S. Qourzal, N. Barka, Spinel ferrites nanoparticles: Synthesis methods and application in heterogeneous Fenton oxidation of organic pollutants – A review, Applied Surface Science Advances, 6 2021, 100145. https://doi.org/10.1016/j.apsadv.2021.100145.

[3] K. Hedayati, Synthesis and Characterization of Nickel Zinc Ferrite Nanoparticles, Journal of Nanostructures, 5(1) 2015, 13-16. https://doi.org/10.7508/JNS.2015.01.002.

[4] M. Asghar, S. Habib, W. Zaman, S. Hussain, H. Ali, S. Saqib, Synthesis and characterization of microbial mediated cadmium oxide nanoparticles, Microscopy Research and Technique, 83(12) 2020, 1574-1584. https://doi.org/10.1002/jemt.23553.

[5] E. Demir, T. Qin, Y. Li, Y. Zhang, X. Guo, T. Ingle, J. Yan, A. I. Orza, A. S. Biris, S. Ghorai, T. Zhou, T. Chen, Cytotoxicity and genotoxicity of cadmium oxide nanoparticles evaluated using in vitro assays, Mutation Research/Genetic Toxicology and Environmental Mutagenesis, 850–851 2020, 503149. https://doi.org/10.1016/j.mrgentox.2020.503149.

[6] A. Mehtab, J. Ahmed, S. M. Alshehri, Y. Mao, T. Ahmad, Rare earth doped metal oxide nanoparticles for photocatalysis: a perspective, Nanotechnology, 33 2022, 142001. https://doi.org/10.1088/1361-6528/ac43e7.

[7] F. Guo, Z. Chen, X. Huang, L. Cao, X. Cheng, W. Shi, L. Chen, Cu_3P nanoparticles decorated hollow tubular carbon nitride as a superior photocatalyst for photodegradation of tetracycline under visible light, Separation and Purification Technology, 275 2021, 119223. https://doi.org/10.1016/j.seppur.2021.119223.

[8] S. Zinatloo-Ajabshir, M. S. Morassaei, O. Amiri, M. Salavati-Niasari, Green synthesis of dysprosium stannate nanoparticles using Ficus carica extract as photocatalyst for the degradation of organic pollutants under visible irradiation, Ceramics International, 46(5) 2020, 6095-6107. https://doi.org/10.1016/j.ceramint.2019.11.072.

[9] Z. Ebrahimi, K. Hedayati, D. Ghanbari, Preparation of hard magnetic $BaFe_{12}O_{19}$–TiO_2 nanocomposites: applicable for photo-degradation of toxic pollutants, Journal of Materials Science: Materials in Electronics, 28, 2017, 13956-13969. https://doi.org/10.1007/s10854-017-7245-3.

[10] A. Kiani, G. Nabiyouni, S. Masoumi, D. Ghanbari, A novel magnetic $MgFe_2O_4$–$MgTiO_3$ perovskite nanocomposite: Rapid photo-degradation of toxic dyes under visible irradiation, Composites Part B: Engineering, 175 2019, 107080. https://doi.org/10.1016/j.compositesb.2019.107080.

[11] X. Yuan, H. Wang, Y. Wu, X. Chen, G. Zeng, L. Leng, C. Zhang, A novel SnS_2–$MgFe_2O_4$/reduced graphene oxide flower-like photocatalyst: Solvothermal synthesis, characterization and improved visible-light photocatalytic activity, Catalysis Communications, 61 2015, 62-66. https://doi.org/10.1016/j.catcom.2014.12.003.

[12] K. Hedayati, D. Ghanbari, M. Kord, M. Goodarzi, (Co, Ag, Ni, Cd, Mn, Cr)-doped PbS photo-catalyst: sonochemical-assisted synthesis of magnetite nanocomposites applicable for elimination of toxic pollutants, Journal of Materials Science: Materials in Electronics, 32 2021, 373–383. https://doi.org/10.1007/s10854-020-04787-5.